10. *Notes on Crustal Deformations in Miyake-sima.*

By Naomi MIYABE,

Earthquake Research Institute.

(Read Nov. 20 1941.—Received Dec. 20, 1941.)

1. In the eruption of Miyake-sima, 1940, the deformation of the earth's surface that accompanied it was found by measuring the horizontal and vertical displacements of triangulation points scattered over this island. The results of an analytical study of these crustal deformations follow.[1)]

2. In this study, the writer first tried to calculate the theoretical values of the displacements, based on the theory of elastic equilibrium with given boundary conditions. In this calculation, the problem was treated as two-dimensional, the elastic strain assumed present only in a horizontal plane.

The problem may be reduced to that of solving the equation of equilibrium

$$\left.\begin{aligned}(\lambda+\mu)\frac{\partial\theta}{\partial x}+\mu\nabla^2 u=0\\ (\lambda+\mu)\frac{\partial\theta}{\partial y}+\mu\nabla^2 v=0,\end{aligned}\right\} \tag{1}$$

where u and v are the x-and y-components of the displacement at point (x, y), and λ, μ are Lame's elastic constants, whence

$$\theta=\frac{\partial u}{\partial x}+\frac{\partial v}{\partial y}. \tag{2}$$

The bounadry conditions to be satisfied are

$$u=0, \quad v=\frac{2v_0}{\pi}\int_0^\infty \frac{\sin a\xi\cos x\xi}{\xi}d\xi \tag{3}$$

at $y=0$ in each quadrant.

On solving the equation, we put

1) The analytical study of the crustal deformation was made by S. Omote. *See Zisin*, **13** (1941), 315~326. This is a supplementary note to Omote's study.

$$\left.\begin{aligned} u&=\phi_1+y\frac{\partial\psi}{\partial x}\\ v&=\phi_2+y\frac{\partial\psi}{\partial y}\end{aligned}\right\} \tag{4}$$

Substituting this relation in equations (1) and (2), and in view of one of the boundary conditions, namely, $u=0$ at $y=0$, we get the relation

$$\theta=\frac{\partial\phi_2}{\partial y}+\frac{\partial\psi}{\partial y}+y\nabla^2\psi\,, \tag{5}$$

and

$$\left.\begin{aligned} \frac{\partial}{\partial x}\left\{\frac{\partial\phi_2}{\partial y}+\frac{\partial\psi}{\partial y}+\frac{2\mu}{\lambda+\mu}\frac{\partial\psi}{\partial y}\right\}&=0\\ \frac{\partial}{\partial y}\left\{\frac{\partial\phi_2}{\partial y}+\frac{\partial\psi}{\partial y}+\frac{2\mu}{\lambda+\mu}\frac{\partial\psi}{\partial y}\right\}&=0\,.\end{aligned}\right\} \tag{6}$$

Hence, while we have on the one hand

$$\frac{\partial\phi_2}{\partial y}=-\frac{\lambda+3\mu}{\lambda+\mu}\frac{\partial\psi}{\partial y}\,,$$

or

$$\phi_2=-\frac{\lambda+3\mu}{\lambda+\mu}\psi\,, \tag{7}$$

on the other, we have from (2)

$$\nabla^2\theta=0 \tag{8}$$

Then ϕ_2 and ψ should satisfy the condition

$$\nabla^2\phi_2=0,\quad \nabla^2\psi=0. \tag{9}$$

The solution of (9) may be written in the form

$$\phi_2=\int_0^\infty e^{-\xi y}(\phi_{2\xi}\cos\xi x+\phi'_{2\xi}\sin\xi x)\,d\xi\,, \tag{10}$$

which should satisfy the boundary condition, i. e., at $y=0$,

$$v=\phi_2=\frac{2v_0}{\pi}\int_0^\infty\frac{\sin a\xi\cos x\xi}{\xi}d\xi\,.$$

The constants in (10) will then become

$$\phi_{2\xi}=\frac{2v_0}{\pi}\frac{\sin a\xi}{\xi},\quad \phi'_{2\xi}=0\,. \tag{11}$$

Thus we have

$$\phi_2=\frac{2v_0}{\pi}\int_0^\infty e^{-\xi y}\frac{\sin a\xi\cos x\xi}{\xi}d\xi \tag{12}$$

and

$$\psi=-\frac{\lambda+\mu}{\lambda+3\mu}\frac{2v_0}{\pi}\int_0^\infty e^{-\xi y}\frac{\sin a\xi\ \mathrm{eos}\ x\xi}{\xi}d\xi\,, \tag{13}$$

that is to say,

$$u=\frac{2v_0}{\pi}\frac{\lambda+\mu}{\lambda+3\mu}\int_0^\infty ye^{-\xi y}\sin a\xi\sin x\xi d\xi \tag{14}$$

and

$$v=\frac{2v_0}{\pi}\int_0^\infty e^{-\xi y}\frac{\sin a\xi\cos x\xi}{\xi}k\xi + \frac{2v_0}{\pi}\frac{\lambda+\mu}{\lambda+3\mu}\int_0^\infty ye^{-\xi y}\sin a\xi\cos x\xi d\xi\,. \tag{15}$$

Since

$$\int_0^\infty e^{-\xi y}\sin a\xi\cos x\xi d\xi=\frac{1}{2}\int_0^\infty\cos(a-x)\xi\cdot e^{-\xi y}d\xi$$

$$-\frac{1}{2}\int_0^\infty\cos(a+x)\xi\cdot e^{-\xi y}d\xi=\frac{1}{2}\left[\frac{y}{(a-x)^2+y^2}-\frac{y}{(a+x)^2+y^2}\right],$$

$$\int_0^\infty e^{-\xi y}\sin a\xi\cos x\xi d\xi=\frac{1}{2}\int_0^\infty\sin(a-x)\xi\cdot e^{-\xi y}d\xi$$

$$+\frac{1}{2}\int_0^\infty\sin(a+x)\xi\cdot e^{-\xi y}d\xi=-\frac{1}{2}\left[\frac{a-x}{(a-x)^2+y^2}+\frac{a+x}{(a+x)2+y^2}\right].$$

$$\int_0^\infty e^{-\xi y}\frac{\sin a\xi\cos x\xi}{\xi}d\xi=\frac{1}{2}\int_0^\infty e^{-\xi y}\frac{\sin(a-x)\xi}{\xi}d\xi$$

$$+\frac{1}{2}\int_0^\infty e^{-\xi y}\frac{\sin(a+x)\xi}{\xi}d\xi=\frac{1}{2}\left[\tan^{-1}\frac{a-x}{y}+\tan^{-1}\frac{a+x}{y}\right],$$

we have for the components of displacements in each quadrant

$$u=\frac{v_0}{\pi}\frac{\lambda+\mu}{\lambda+3\mu}y^2\left[\frac{1}{(a-x)^2+y^2}-\frac{1}{(a+x)^2+y^2}\right] \tag{16}$$

$$v=\frac{v_0}{\pi}\left[\tan^{-1}\frac{a-x}{y}+\tan^{-1}\frac{a+x}{y}\right]$$

$$-\frac{v_0}{\pi}\frac{\lambda+\mu}{\lambda+3\mu}y\left[\frac{a-x}{(a-z)^2+y^2}+\frac{a+x}{(a+x)^2+y^2}\right] \qquad (17)$$

3. In studying the crustal deformation in Miyake-sima by using the results of the foregoing calculation, the cracks that accompanied the eruption is expressed schematically.

It was reported[2] that, at the time of eruption, several new craters were formed on the north-eastern slope of the Miyake-sima volcano, distributed on a line the trend of which is N 72° E, radially from the Oyama crater, lying in the centre of Miyake-sima. This direction was chosen for the x-axes in the present analytical study, and the perpendicular to it for the y-axis. The origin of the coordinates was taken at the point where the x-axis intersects the shore-line of the

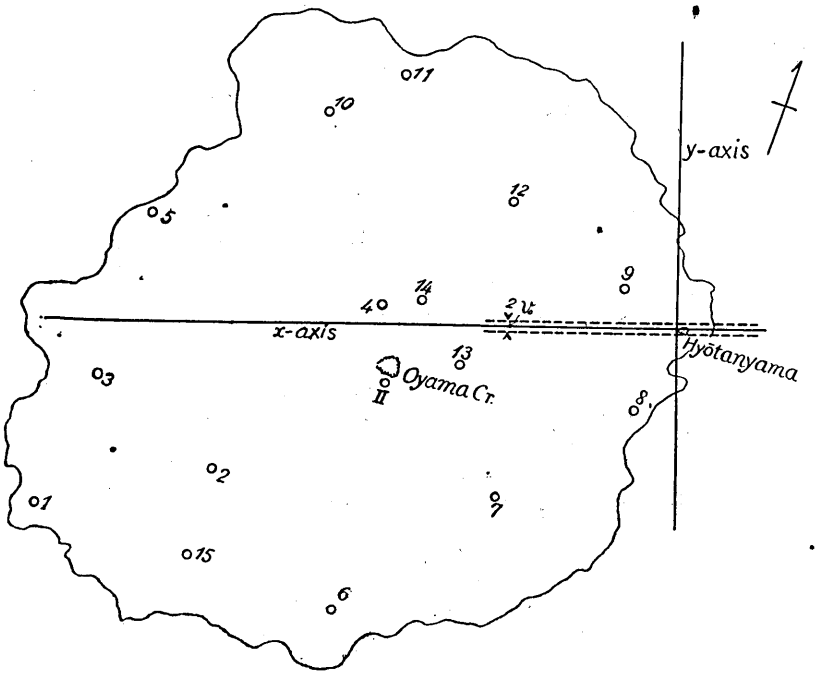

(Numerals against points designate the number of triangulation points.)

Fig. 1 Distribution of triangulation points.

island, where the Hyōtan-yama crater was formed at the time of eruption. Along this x-axis, i.e., on a part of the surface from this origin to the westernmost crater, a straight crack was formed, pushing out

2) H. TSUYA, *Bull. Earthq. Res. Inst.*, **19** (1941), 263~294.

towards both sides of the crack, its width being $2v_0$. The distance between Hyōtanyama, the origin of the coordinates, and the westernmost crater is taken as a. On the eastern side of the y-axis, a similer crack also formed. The coordinate axes and the crack are shown in Fig. 1, in which the distribution of triangulation points is also shown.

Since the coordinate axes are rotated 18,° counterclockwise, compared with the coordinate axes in which the eastward and northward directions are taken as x- and y- axes, respectively, and to which the components of displacements[3] are referred, the components of horizontal displacements should be reduced to some such form as

$$\left.\begin{aligned} u' &= u\cos 18^\circ + v\sin 18^\circ \\ v' &= -u\sin 18^\circ + v\cos 18^\circ \end{aligned}\right\} \tag{18}$$

where u, v are values as referred to the ordinary coordinate axes and u', v' the revised values of components of displacements as referred to the rotated coordinate axes.

Table I. Revised Horizontal Displacements.

Triangulation Points	u (cm)	v (cm)
II	−34	− 2
1	0	0
2	−22	2
3	−13	−11
4	−26	0
5	−23	−14
6	−25	−19
7	−34	−54
8	−31	−84
9	3	108
10	−62	10
11	−68	20
12	−61	61
13	−44	− 4
14	−16	− 9
15	−22	0

Table II. Revised Coordinates of Triangulation Points.

No. of Triangulation pts.	x	y
	km	km
II	−3·84	−0·75
1	−8·50	−2·45
2	−6·15	−1·95
3	−7·71	−0·73
4	−3·92	0·28
5	−7·02	1·45
6	−4·50	−3·78
7	−2·33	−2·25
8	−0·55	−1·07
9	−0·70	0·55
10	−4·70	2·82
11	−3·70	3·34
12	−2·20	1·66
13	−2·90	−0·50
14	−3·42	0·35
15	−6·46	3·11

The reduced values of the components of the horizontal displacements are given in Table I.

3) *Bull. Earthq. Res. Inst.*, **19** (1941), 544~547.

The coordinates of the triangulation points with reference to the new coordinate axes as measured on the map and given in Table II.

Theoretical values of components of horizontal displacements were calculated by using (16) and (17), given in the preceding paragraph for cases of $\lambda=\mu$ and $\frac{\lambda}{\mu}=\infty$ respectively, i. e., for the case in which the crust is perfectly elastic and for that in which it is incompressible, taking the value of $2v_0$ as 240 cm. The results are given in Table III, in which values of δu and δv, i.e., the difference between the observed and calculated components of horizontal displacements are also shown.

Table III. Calculated Horizontal Displacements.

Triangulation Points.	Case $\lambda=\mu$				Case $\frac{\lambda}{\mu}=\infty$			
	u(cm)	v(cm)	δu	δv	u(cm)	v(cm)	δu	δv
II	− 2	−12	−32	10	− 5	−15	−29	−13
1	0	0	0	0	0	0	0	0
2	− 1	− 5	−21	7	− 3	− 6	−19	8
3	2	5	−15	−16	3	7	−16	−18
4	1	17	−27	−17	3	21	−29	−21
5	1	−12	−19	−32	1	24	−24	−38
6	− 9	−32	−16	13	−17	−13	− 8	− 6
7	−14	−29	−20	−25	−27	−17	− 7	−37
8	0	−64	−31	−20	− 1	−47	−30	−37
9	1	104	2	4	2	98	1	10
10	− 7	32	−55	−22	−15	38	−47	−28
11	−11	35	−42	−15	−22	36	−46	−16
12	−10	53	−51	8	−20	47	−41	14
13	−10	−30	−34	26	−19	−31	−25	27
14	0	26	−16	−35	− 1	34	−15	−43
15	− 3	− 7	−19	7	− 7	− 7	−15	7

It will be seen from this result that the calculated displacements for the case in which the crust was assumed incompressible are closer to the actual values of components of horizontal displacements than those calculated for the case in which the crust is assumed perfectly elastic. The theoretical values of components of the horizontal displacements were then calculated for various values of $2v_0$ for the case of an incompressible crust and the results compared with the actual values of the components of horizontal displacements.

The residuals δu and δv were worked out and the sum of the squares of these residuals, i. e., the value of $\sum\{(\delta u)^2+(\delta v)^2\}$ obtained

for each different value of v_0 and plotted against v_0, as shown in Fig. 2.

It was thus found that the calculated values of components of horizontal displacements approach nearest the actual when v_0 is assumed to be 120—140 cm.

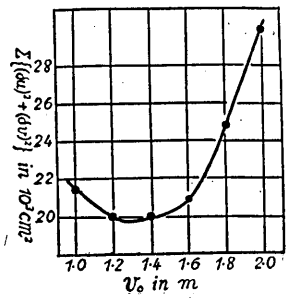

Fig. 2.

It is a matter for further discussion whether the value of v_0 that gives the least value of $\sum\{(\delta u)^2+(\delta v)^2\}$ is the most probable one or not. However, the value of 120 cm is taken as the most probable value of v_0, and referring to this value, the residuals, i. e., the difference of the observed horizontal displacements from those calculated, were worked out and their distributions discussed. In Fig. 3, the observed and calculated horizontal displacements of triangulation points are shown by the full and dotted arrows.

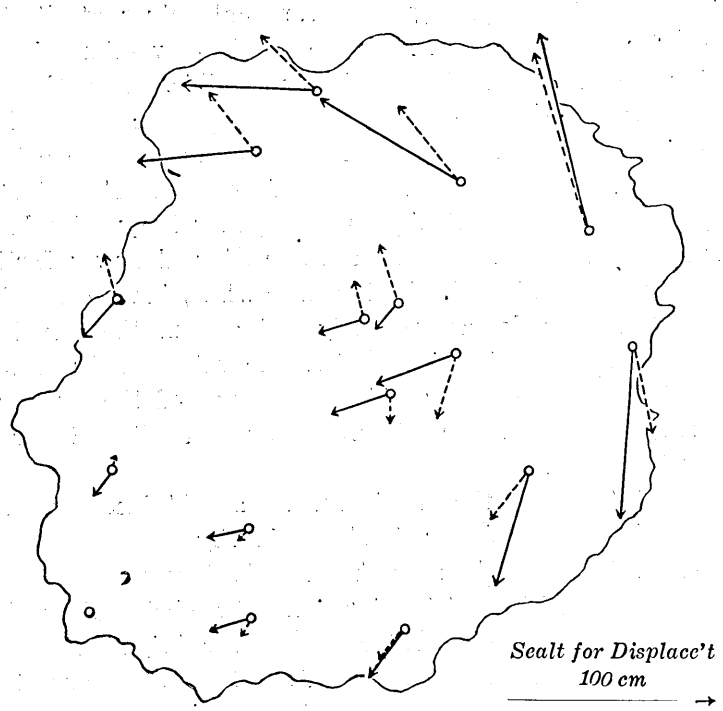

(full arrows=actual, dotted arrows=calculated.)
Fig. 3. Distribution of horizontal displacements.

The residuals of the horizontal displacements thus worked out

consist of errors accidental and systematic. One of these systematic errors is such that its amount is usually believed to increase with increasing distance from the point of reference. As the point of reference in this case, triangulation point 1 was selected. We have for the components of these errors the expressions

$$\left.\begin{aligned} u_e &= Ax - By \\ v_e &= Ay + Bx \end{aligned}\right\} \tag{19}$$

in which x and y are coordinates of the triangulation point referred to triangulation point 1 in this case, and A and B are constants determined by means of the data of residuals by the method of least squares, namely $A = -0.881 \times 10^{-5}$ $B = 1.085 \times 10^{-5}$

Several other sources of deviations, or residuals, could also be pointed out, one being the systematic errors that arise from improper assumptions made in computing the theoretical values of displacement components, for example, in treating the problem two-dimensionally and in assuming the earth's crust to be incompressible. The effect of local deformations and the accidental errors are also sources of deviation.

Since a number of sources of residuals can thus be pointed out, it might be said that the determination of constants A and B in the above expression by the method of least squares is questionable. This is also one reason that the assumed value of v_0 deserves further discussion, as already mentioned. In the meanwhile, however, seeing that the above calculations do not seriously differ from the actual manner of deformation, the second residuals, i. e., the values of $\delta u - u_e$, $\delta v - v_e$, are regarded as consisting of accidental errors and the components of local deformations, the cause of which was not allowed for in the foregoing calculations.

The distribution of the displacements as obtained by combining the values of $\delta u - u_e$ and $\delta v - v_e$ is shown in Fig. 4.

From all this, it will be seen that the displacements of triangulation points 4, 15, 14, II are fairly large, the three being directed toward the crater of Oyama, the central crater of the Miyake-sima volcano. Such manner of crustal deformation might have been caused by the volcanic activity of Oyama, whose activity had been reported several days after the eruption on the northeastern side of Miyake-sima.

A similar mode of deformation may also be seen from the analysis of the vertical displacements of the triangulation points.

4. A glance at the distribution of the vertical displacements of triangulation points shows that Miyake-sima island as a whole tilted westwards. This general tilt may consist of acute deformation that accom-

panied the volcanic eruption and a secular deformation that has been accumulating for scores of years. In a study of the crustal deformation that followed the volcanic eruption, the chronic general tilt ought

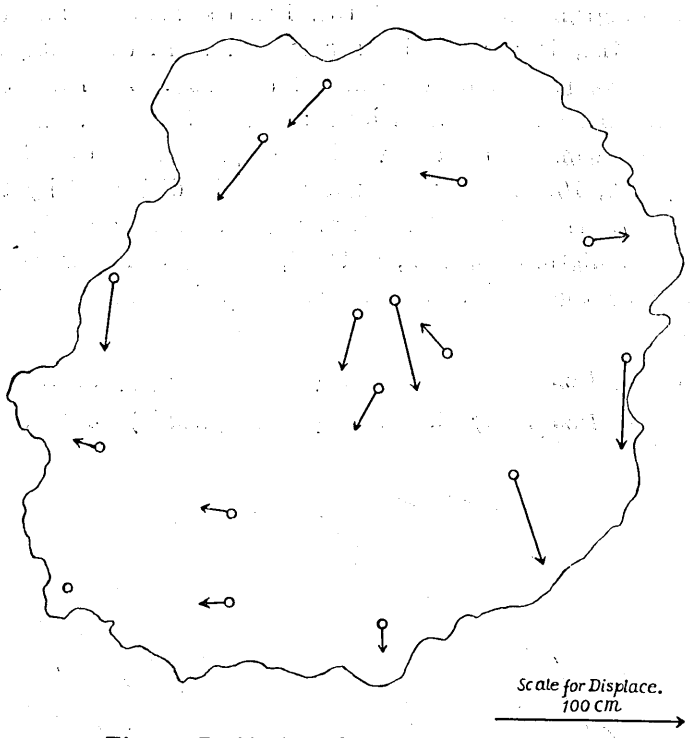

Fig. 4. Residuals of horizontal displacements.

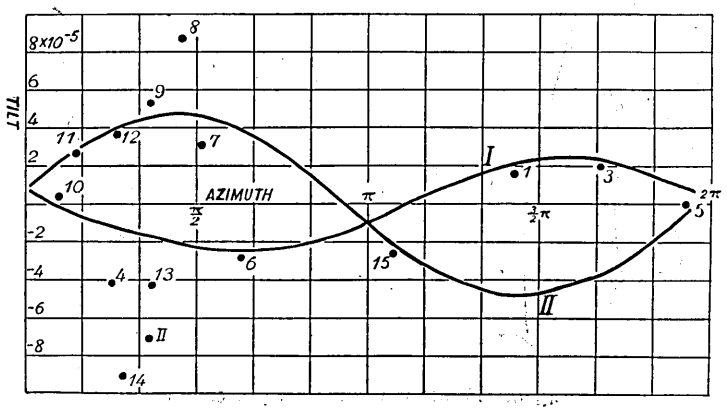

Fig. 5.

rather to be excluded. In order to exclude this general tilt, the following procedure was taken.

The apparent tilt in the azimuth connecting the two triangulation points was calculated, and this apparent tilt plotted against the azimuth, as shown in Fig. 5.

In this diagram, the general tilt, i.e., the azimuth and the magnitude of the tilt, is denoted by a sine-curve. In this case, however, such a sine-curve cannot be determined uniquely. At least two sine-curves can be drawn, designated by I and II. Sine-curve I represents the tilt as determined by the vertical displacements of triangulation points 2, 1, 3, 6, 10, which were not seriously disturbed by the eruption, while curve II represents the tilt as determined by vertical displacements of triangulation points 2, 5, 9, 11, 12, 15, which were disturbed more or less by the eruption. The general tilts represented by these sine-curves are

$$\text{I:}\quad \theta_m \text{ (azimuth)} = 108°, \qquad \varphi_m \text{ (magnitude)} = 2.4 \times 10^{-5}$$
$$\text{II:}\quad \theta_m \text{ (azimuth)} = 260°, \qquad \varphi_m \text{ (magnitude)} = 4.8 \times 10^{-5}$$

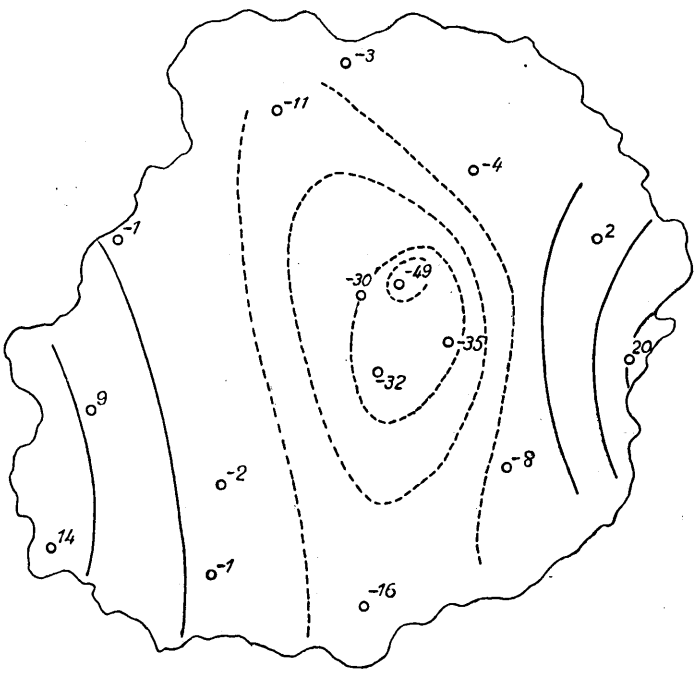

Fig. 6. Reduced vertical displacements.

Thus curve I shows the south-eastward tilt and curve II the westward tilt. If we assume the tilt represented by curve II to be the general tilt and subtract the effect of this general tilt from the actual

vertical displacements of the triangulation points, the distribution of the vertical displacements thus corrected is as that shown in the annexed figure in which, in the central part of Miyake-sima around the Oyama crater, the earth's surface was found to have subsided, both the east and west sides of the island being elevated relatively.

From this distribution of corrected vertical displacements, the crustal deformation is believed to have occurred in association with the activity of the Oyama crater of the Miyake-sima volcano, as already found from an anaytical study of the horizontal displacements.

The assumed general tilt represented by curve II, Fig. 5, may contain the components of vertical displacements due to the volcanic eruption on the north-eastern slope of the mountain.

In Column III of Table IV, the corrected vertical displacements, assuming the curve II of Fig. 5 to represent the general tilt, are shown.

In Column II of this Table, are shown the vertical displacements, corrected on the assumption that the tilt represented by curve I, Fig. 5, represents the general tilt.

Table IV. Reduced vertical Displacements.

Triangulation Points	W_1(cm)	W_2(cm)
II	−15	−32
1	− 3	14
2	− 2	− 2
3	1	9
4	−14	−30
5	− 6	− 1
6	− 3	−16
7	20	− 8
8	60	20
9	41	2
10	0	−11
11	16	− 3
12	25	− 4
13	−12	−35
14	−29	−49
15	− 5	− 1

As will be seen from this Table, the corrected vertical displacements in Column III, the corrections for which are based on the general tilt represented by curve II, Fig. 5, are so related to the calculated horizontal displacements that the larger vertical displacements point to smaller horizontal displacements. On the other hand, however, in the vertical displacements given in Column II of the Table, the larger values of the vartical displacements point to larger values of the calculated horizontal displacements.

The relations between the calculated horizontal displacements and the corrected vertical displacements, for which the corrections are calculated by assuming the tilt represented by curve I as being the general tilt, is shown in the annexed figure.

Omitting the points that show the relation between the calculated

vertical and horizontal displacements of triangulation points 14, 4, 13, II, and 8, the relation is expressible by a curve, as shown in Fig. 7. The displacements of triangulation points 14, 4, 13, and II are seen to have been greatly affected by the volcanic activity of Oyama crater, as already referred to, the value of the corrected vertical displacements of the triangulation point 8 being exceptionally large. These are the reasons for the omission in Fig. 7, of the points corresponding to these triangulation points.

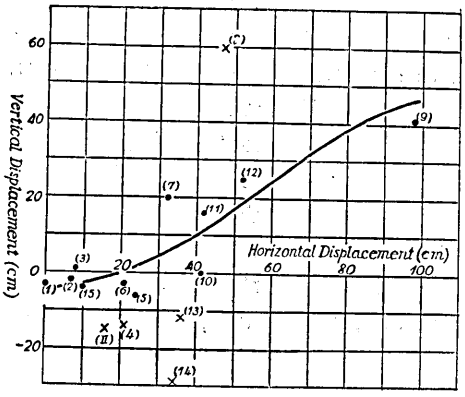

Fig. 7.

This fact may suggest that the crustal deformation that accomapanied the volcanic eruption was caused by an abrupt upward movement of the subterranean lava. Hence, in calculating the theoretical values of displacements, the boundary condition should be taken so that they shall express the process of eruption mentioned above which however could not be easily expressed in mathematical form.

5. The results of the present study may be summarized as follows:

(i) The dispribution of the horizontal displacements in Miyake-sima caused by the 1940 eruption is expressible approximately by the deformation that would be expected from such mode of crustal movement that the crust was pushed outward as the result of a crack, 240 cm wide, opening on the northeastern slope of Miyake-sima volcano. A number of explosion craters are distributed on this line of crack.

(ii) Comparisons of the deviations in horizontal displacements worked out with the aid of the observed and calculated values suggests that, accompanying the volcanic activity of the Oyama crater at the center of the volcano, a local converging deformation occurred.

(iii) From analytical studies of the vertical displacements of triangulation points, it was also noticed that, associated with the volcanic activity of Oyama crater, the region around this crater subsided.

It is hoped that the results of analytical study of the crustal deformation in Miyake-sima given in this paper will stimulate further investigations and also theoretical treatment of more general cases having more complicated boundary conditions.

In conclusion, the writer wishes to express his sincere thanks to

the Department of Education for the grant of a Scientific Research Encouradgment Fund for prosecuting this study. The writer's thanks are also due to Miss Maeda for assistance in calculating the numerical values of the theoretical displacements.

---

10. 三宅島の地殻變形

地震研究所 宮部直巳

三宅島の噴火（昭和 15年 7月 12日）に伴つて生じた地殻の變形は，三角測量の實施せられたる結果求められた所の島内にある 16 個の三角點の水平及び垂直方向の移動量によつて示された．

この移動量について調べた結果次のやうなことを指摘することが出來る．

（i） 水平移動量だけを取出して考へることが許されるならば，三宅島東北山腹に西南から北東の方向に生じた火口列に沿ひ地表面が 2·4 m 程の幅に開口した爲の地殻の 彈性的な變形だとして，ある程度まで說明することが出來る．然し，中央部の雄山火口周邊に於ける稍々異常的な變動が殘る．

(ii) 垂直變動量につき，噴火の影響と思はれる東西方向の著しい傾斜の影響を除いてみると，中央部の雄山周邊地域が著しく低下してゐることが知れる．
